

Review

# The Use of Artificial Intelligence and Satellite Remote Sensing in Land Cover Change Detection: Review and Perspectives

Zhujun Gu <sup>\*,†</sup> and Maimai Zeng <sup>†</sup>

Pearl River Water Resources Research Institute, Pearl River Water Resources Commission, Guangzhou 510610, China; zengmimai@pearlwater.gov.cn

\* Correspondence: guzhujun@pearlwater.gov.cn

<sup>†</sup> These authors contributed equally to this work.

**Abstract:** The integration of Artificial Intelligence (AI) and Satellite Remote Sensing in Land Cover Change Detection (LCCD) has gained increasing significance in scientific discovery and research. This collaboration accelerates research efforts, aiding in hypothesis generation, experiment design, and large dataset interpretation, providing insights beyond traditional scientific methods. Mapping land cover patterns at global, regional, and local scales is crucial for monitoring the dynamic world, given the significant impact of land cover distribution on climate and environment. Satellite remote sensing is an efficient tool for monitoring land cover across vast spatial extents. Detection of land cover change through satellite remote sensing images is critical in influencing ecological balance, climate change mitigation, and urban development guidance. This paper conducts a comprehensive review of LCCD using remote sensing images, encompassing exhaustive examination of satellite remote sensing data types and contemporary methods, with a specific focus on advanced AI technology applications. Furthermore, the study delves into the challenges and potential solutions in the field of LCCD, providing a comprehensive overview of the state of the art, offering insights for future research and practical applications in this domain.

**Keywords:** land cover; artificial intelligence; change detection; satellite remote sensing images; ecological protection



**Citation:** Gu, Z.; Zeng, M. The Use of Artificial Intelligence and Satellite Remote Sensing in Land Cover Change Detection: Review and Perspectives. *Sustainability* **2024**, *16*, 274. <https://doi.org/10.3390/su16010274>

Academic Editors: Hong Tang, Jing Wei and Naisen Yang

Received: 7 November 2023

Revised: 11 December 2023

Accepted: 21 December 2023

Published: 28 December 2023



**Copyright:** © 2023 by the authors. Licensee MDPI, Basel, Switzerland. This article is an open access article distributed under the terms and conditions of the Creative Commons Attribution (CC BY) license (<https://creativecommons.org/licenses/by/4.0/>).

## 1. Introduction

Land cover refers to the various physical cover types on the Earth's surface, such as lakes, forests, grasslands, agricultural land, rivers, and urban land [1]. Human activities such as urbanization, mining, agricultural expansion, and deforestation have led to significant land cover changes, resulting in desertification and biodiversity loss, which have severe impacts on terrestrial ecosystems [2–7]. The increasing global population and urbanization have led to the conversion of natural forests and lakes into grasslands, cultivated land, and urban areas, causing substantial environmental changes [8]. Therefore, the protection of land resources is imperative and has driven extensive research related to land cover change detection (LCCD).

The impacts of land cover changes are far-reaching, particularly on natural resources, and these rapidly increasing changes have raised significant concerns about their potential effects on global environments. LCCD plays a crucial role in preserving ecological balance [9–12], disaster management [13–20], fire detection [21], urban development monitoring [22–31], resource management [32–34], ensuring food supply [35,36], addressing climate change [37], and assessing ecosystem health [38–41].

The emergence of deep learning in the early 2010s significantly expanded the scope and ambition of scientific discovery processes [1]. Artificial intelligence (AI) is increasingly employed across scientific disciplines to integrate massive datasets, refine measurements, guide experimentation, explore the space of theories compatible with the data, and provide actionable and reliable models integrated with scientific workflows for autonomous

discovery. The power of AI methods has vastly increased since the early 2010s because of the availability of large datasets aided by fast and massive parallel computing and storage hardware (graphics processing units and supercomputers) coupled with new algorithms. The latter includes deep representation learning, particularly multilayered neural networks capable of identifying essential, compact features that can simultaneously solve many tasks that underlie a scientific problem. Of these, geometric deep learning has proven to be helpful in integrating scientific knowledge, presented as compact mathematical statements of physical relationships, prior distributions, constraints and other complex descriptors, such as the geometry of atoms in molecules.

The use of AI and satellite remote sensing for LCCD has several key benefits. Firstly, tracking land cover changes allows for the assessment of the health and stability of natural ecosystems, which is vital for preserving biodiversity, reducing deforestation, managing wetland degradation, combating desertification, and maintaining the health of aquatic and marine ecosystems. Secondly, understanding land cover changes is closely linked to efforts to adapt to and mitigate climate change. Monitoring changes in land cover helps in comprehending the impact of activities such as deforestation, land conversion, and urban expansion on carbon storage and the climate system. Thirdly, rapid population growth and urbanization necessitate a comprehensive understanding of land use patterns. By observing urban expansion, land development, and changes in land use, urban planners can better design infrastructure, provide public services, meet the evolving needs of growing urban populations, and ensure sustainability. Fourthly, agriculture is a fundamental component of global food security, and understanding agricultural land use, crop production, and soil fertility is critical for decision-making, agricultural management, and food security.

Traditionally, land cover information was obtained through manual monitoring and observation, such as walking or land vehicle measurements, which is time-consuming and costly, especially for large and remote areas. However, with the advancement of remote sensing technology, a large number of remote sensing images containing ground information have been acquired, greatly alleviating this situation. Satellite remote sensing, in particular, has emerged as a powerful tool for detecting changes in ground cover. Satellite remote sensing methods capture ground cover images by equipping satellites with sensors, these methods can continuously capture ground cover images at a relatively lower cost and with wide coverage, a long coverage period, and relatively convenient data processing [42–44]. Therefore, the use of satellite remote sensing images for detecting changes in ground cover is preferred over aerial and ground remote sensing images. In recent decades, the utilization of satellite remote sensing data for quantifying ground cover changes and their impact on the Earth's surface over time has become a hot research topic in the field. The satellite remote sensing images can be obtained using optical and radar sensors. And with the development of technological, cost down, statistical learning and AI, particularly the advancement of vision transformers, generative adversarial networks (GANs), and large-scale visual segmentation models, has led to a plethora of methods for LCCD.

At present, there are several review articles concerning land cover or change detection [45–49]. Specially, refs. [45,46] focused on common methods of change detection using remote sensing rather than providing a comprehensive review of LCCD methods. Ref. [47] synthesized and summarized the methods of LCCD using very high-resolution remote sensing images. Ref. [48] reviewed the methods of LCCD using GIS and remote sensing data. Ref. [49] considering the applicability and feasibility of land use and land cover change modelling in a wide range of agricultural, environmental, and ecological problems and emphasis discusses the classification and change of land use. In contrast to these existing works, this paper offers a comprehensive review of LCCD methods utilizing AI and satellite remote sensing, specifically delving into the most advanced AI technology applied in LCCD. Furthermore, we conduct an analysis of the current challenges in the field of LCCD and propose potential directions for future research. Overall, this paper presents several key contributions:

1. This paper offers a comprehensive review of current research in LCCD using artificial intelligence (AI) and satellite remote sensing. It introduces a generic taxonomy to categorize existing works based on challenges in remote image sensing analysis, types of land cover, machine learning models for classification and prediction, and data fusion schemes. The review is based on academic databases, focusing on peer-reviewed journal articles and conference publications.
2. This paper discusses the significant applications of AI and remote sensing image analysis for LCCD, while also identifying the open challenges associated with these applications.
3. This paper conducts a detailed analysis and discussion of the surveyed works, emphasizing the importance of employing AI and satellite remote sensing images for LCCD, highlighting limitations and drawbacks, and addressing current challenges.
4. This paper proposes future research directions to enhance the efficiency, reliability, and accuracy of detecting environmental impacts using AI and remote sensing images. These directions include leveraging explainable AI for better understanding AI model outcomes, utilizing point-clouds for improved description of objects and scenes in satellite images, and employing advanced large language model (LLM) based fusion techniques to develop smart LCCD mechanisms.

In conclusion, this paper comprehensively reviews the methods for assessing LCCD using artificial intelligence and satellite remote sensing, specifically focusing on the most advanced AI technology applied in LCCD. In addition, we analyze the current challenges in the field of LCCD and potential directions for future research. The organization of this article is as follows: Section 2 introduces the satellite remote sensing imagery currently used for LCCD. We review the methods based on satellite remote sensing imagery in Section 3. In Section 4, we discuss the challenges faced in LCCD in detail and provide possible solutions. Finally, in Section 5, we summarize the entire article.

## 2. Satellite Remote Sensing and Datasets

With the continuous advancement of satellite remote sensing technology, access to a wealth of satellite remote sensing data related to land cover has significantly propelled the development of the field of land cover detection. Currently, satellite remote sensing data can be broadly categorized into two major classes based on the different electromagnetic spectral ranges utilized: optical remote sensing imagery and radar remote sensing imagery. We introduce the principles of acquiring these two types of remote sensing imagery, their advantages and disadvantages, and the relevant satellites involved. Additionally, we introduce the commonly used datasets for LCCD using AI technology.

### 2.1. Optical Remote Sensing Imagery

Because of its higher resolution, optical remote sensing imagery is widely utilized in fields such as LCCD, vegetation monitoring, urban planning, environmental monitoring, and archaeology. Typically, optical remote sensing imagery is obtained using optical sensors, including cameras, spectrometers, and multispectral sensors, which utilize wavebands of visible light and infrared radiation. It is a passive way to obtain data, and Figure 1 depicts the principle of acquiring optical remote sensing imagery. The capture of optical remote sensing imagery depends on the light.

Depending on the type and number of spectral bands, optical remote sensing imagery can be categorized into multispectral, hyperspectral, visible light, and panchromatic remote sensing imagery. In the field of LCCD, the primary types used are multispectral and hyperspectral remote sensing imagery. Multispectral data can distinguish geographical targets based on spectral information and is relatively cost-effective. Hyperspectral data, with narrower bands and higher resolution, is more expensive. Additionally, atmospheric conditions, light, and clouds can significantly impact the remote sensing images obtained by optical sensors [50]. Nevertheless, compared with radar images, remote sensing images obtained by optical sensors are easier to interpret directly and possess high spatial reso-

lution. Therefore, under specific atmospheric conditions and illumination, optical remote sensing data remains the primary data source for LCCD.

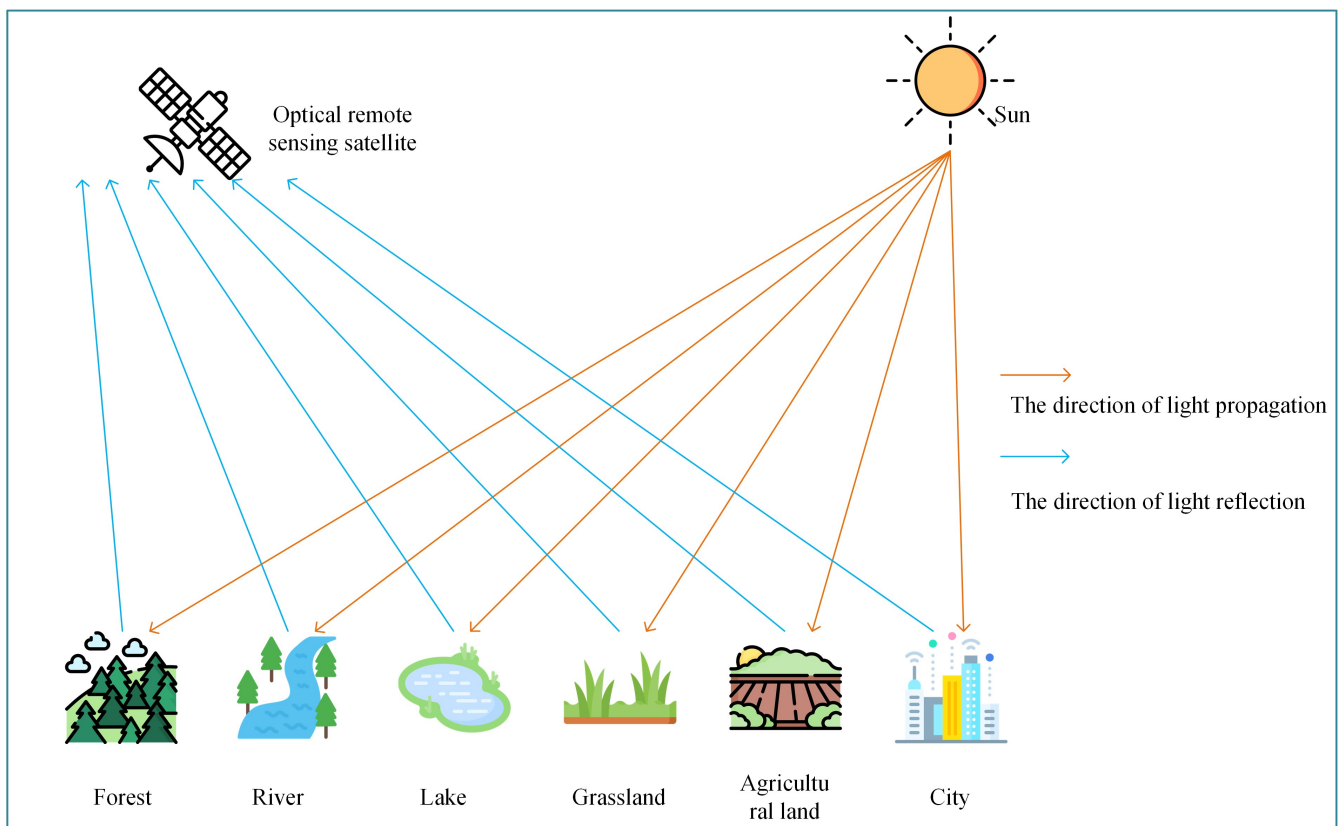


**Figure 1.** Optical Remote Sensing Image Acquisition Principle.

Since the launch of the first land observation satellite, Landsat-1, in 1972, numerous satellites dedicated to land observation have been launched. Here, we will primarily introduce some common optical remote sensing satellites for LCCD:

- (1) **Landsat Satellite Series:** Landsat is a series of satellites operated by the United States Geological Survey (USGS), providing multispectral remote sensing data over many years. The Landsat series, spanning from Landsat 1 through Landsat 9, offers images with varying resolutions and spectral bands. These data are suitable for applications such as land cover classification, resource management, and environmental monitoring.
- (2) **Sentinel Satellite Series:** Sentinel is a series of satellites from the European Space Agency (ESA), with Sentinel-2 satellites providing high-resolution multispectral data. These data are used for land cover classification, vegetation monitoring, agricultural management, among other applications. Sentinel-2 is part of the Copernicus program.
- (3) **MODIS (Moderate Resolution Imaging Spectroradiometer):** MODIS is a sensor carried on NASA's Terra and Aqua satellites, providing moderate-resolution multispectral data for global meteorological, environmental, vegetation, and ocean monitoring.
- (4) **WorldView Satellite Series:** The WorldView satellite series, operated by DigitalGlobe, offers high-resolution optical remote sensing data, supporting applications such as high-precision map-making, urban planning, monitoring, and national security.
- (5) **QuickBird Satellite:** QuickBird, a high-resolution satellite by DigitalGlobe, provides multispectral and panchromatic image data, suitable for urban planning, natural resource management, and agricultural monitoring.
- (6) **Pleiades Satellite Series:** The Pleiades satellite series, a collaboration between the French National Space Research Centre (CNES) and Airbus Defense and Space, of-

fers high-resolution optical images for urban planning, military intelligence, and environmental monitoring.

- (7) SPOT Satellite Series: The SPOT (Satellite Pour l'Observation de la Terre) series, operated by the French aerospace company CNES, provides high-resolution optical image data for land cover classification, resource management, and environmental monitoring.
- (8) IKONOS Satellite: IKONOS was the first commercial high-resolution satellite, delivering multispectral and panchromatic imagery widely used in urban planning, agriculture, and environmental monitoring.

As a result of the open availability of remote sensing image data from Landsat, MODIS, and Sentinel satellites, the majority of LCCD methods depend on the optical remote sensing image data offered by these three satellite series.

## 2.2. Radar Remote Sensing Imagery

Synthetic aperture radar (SAR) is a special radar remote sensing technology that can obtain high-resolution earth observation images. Therefore, the radars carried by satellites are SAR at present. Figure 2 illustrates the principle of acquiring radar remote sensing images. Its significant features include the active emission of electromagnetic waves, enabling all-day and all-weather observations of the Earth independent of sunlight and weather conditions. It also has a certain penetration capability through clouds, fog, light rain, vegetation, and dry materials. Additionally, by adjusting the optimal observation angle, it can effectively detect the spatial morphological characteristics of target objects. However, SAR data can be subject to electromagnetic interference, susceptible to geometric distortion, complex and difficult to interpret, and expensive to develop and maintain [50]. Therefore, several LCCD methods have been proposed to solve these problems, thus improving the accuracy of LCCD. We will briefly introduce some satellites that provide radar remote sensing images as follows.

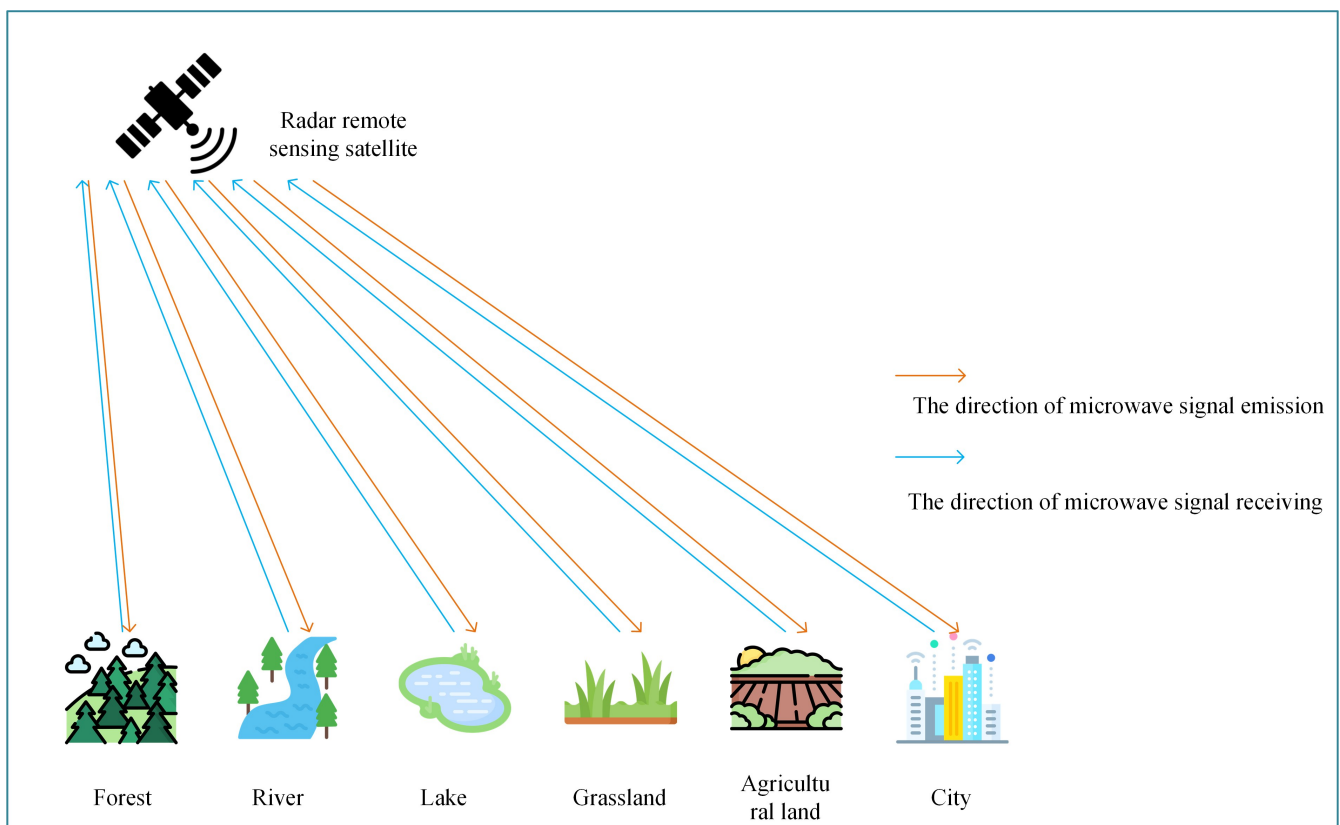


Figure 2. Radar Remote Sensing Image Acquisition Principle.

- (1) Sentinel-1 Satellite: Sentinel-1 is a series of radar remote sensing satellites operated by the European Space Agency (ESA). It offers high-resolution synthetic aperture radar (SAR) data and is widely used in surface monitoring, geological exploration, disaster monitoring, and more.
- (2) RADARSAT Satellite Series: RADARSAT is a series of radar remote sensing satellites operated by the Canadian Space Agency (CSA). These satellites provide multi-mode radar data and are employed in applications such as glacier monitoring, maritime safety, and resource management.
- (3) TerraSAR-X Satellite: TerraSAR-X is a satellite resulting from a collaboration between the German Aerospace Center (DLR) and Airbus Defense and Space. It offers high-resolution X-band SAR data, suitable for applications like urban planning, military intelligence, and geological research.
- (4) COSMO-SkyMed Satellite Series: COSMO-SkyMed is a series of radar remote sensing satellites operated by the Italian Space Agency (ASI). They provide high-resolution SAR data for applications including emergency response, land monitoring, and agriculture.

These radar remote sensing satellites contribute significantly to various fields by providing valuable data under adverse weather and lighting conditions.

### 2.3. Datasets

In this section, we describe in detail the commonly publication used optical remote sensing datasets and SAR datasets for LCCD. Table 1 shows the details of these public datasets.

**Table 1.** The details of the commonly used public datasets for LCCD.

Dataset	Type	Resolution (m)	Class	The Number of Samples
Multispectral-Abudhabi [51]	Optical	10	changed /unchanged	2700 7500
Multispectral-Saclay [51]	Optical	10	changed /unchanged	500 4900
Hyperspectral-River [51,52]	Optical	30	changed /unchanged	2200 5000
Hyperspectral-Farmland [51,53]	Optical	30	changed /unchanged	2000 2500
PolSAR-San Francisco1 [51]	SAR	1.66	changed /unchanged	810 2400
PolSAR-San Francisco2 [51]	SAR	1.66	changed /unchanged	400 700

Multispectral-Abudhabi and Multispectral-Saclay are the typically multispectral datasets. Multispectral-Abudhabi consists of the image of Abudhabi, United Arab Emirates (UAE) on 20 January 2016 and 28 March 2018. The images of Multispectral-Saclay were captured over the Saclay region in Paris, France, on 15 March 2016 and 29 October 2017. Hyperspectral-River and Hyperspectral-Farmland are the hyperspectral datasets. The images Hyperspectral-River were obtained over Jiangsu Province, China, on 3 May 2013 and 31 December 2013, and Hyperspectral-Farmland depict an irrigated agricultural field in Hermiston City in Umatilla County, Oregon, OR, USA, and were acquired on 1 May 2004, and 8 May 2007, respectively. PolSAR-San Francisco1 and PolSAR-San Francisco2 were acquired in San Francisco city on 18 September 2009 and 11 May 2015, the public dataset of SAR for LCCD. These public datasets have greatly promoted the development of AI technology and satellite remote sensing in the field of LCCD.

### 3. Literature Review of LCCD

To ensure that our review reflects the current state of research, we conducted a search on the Web of Science website using keywords “land cover change detection”, “land cover image segment”, “land cover satellite remote sensing”, “land cover artificial intelligence”, and “land cover large model” to retrieve relevant papers published from 2017 to 2023. Initially, we obtained 383 papers and subsequently excluded literature that was not pertinent to the topic, resulting in a final selection of 73 papers. As depicted in Figure 3, the distribution of these papers by year indicates a growing interest among scholars in land cover change detection based on satellite remote sensing data and artificial intelligence techniques in recent years. This suggests that this field continues to hold significant value.

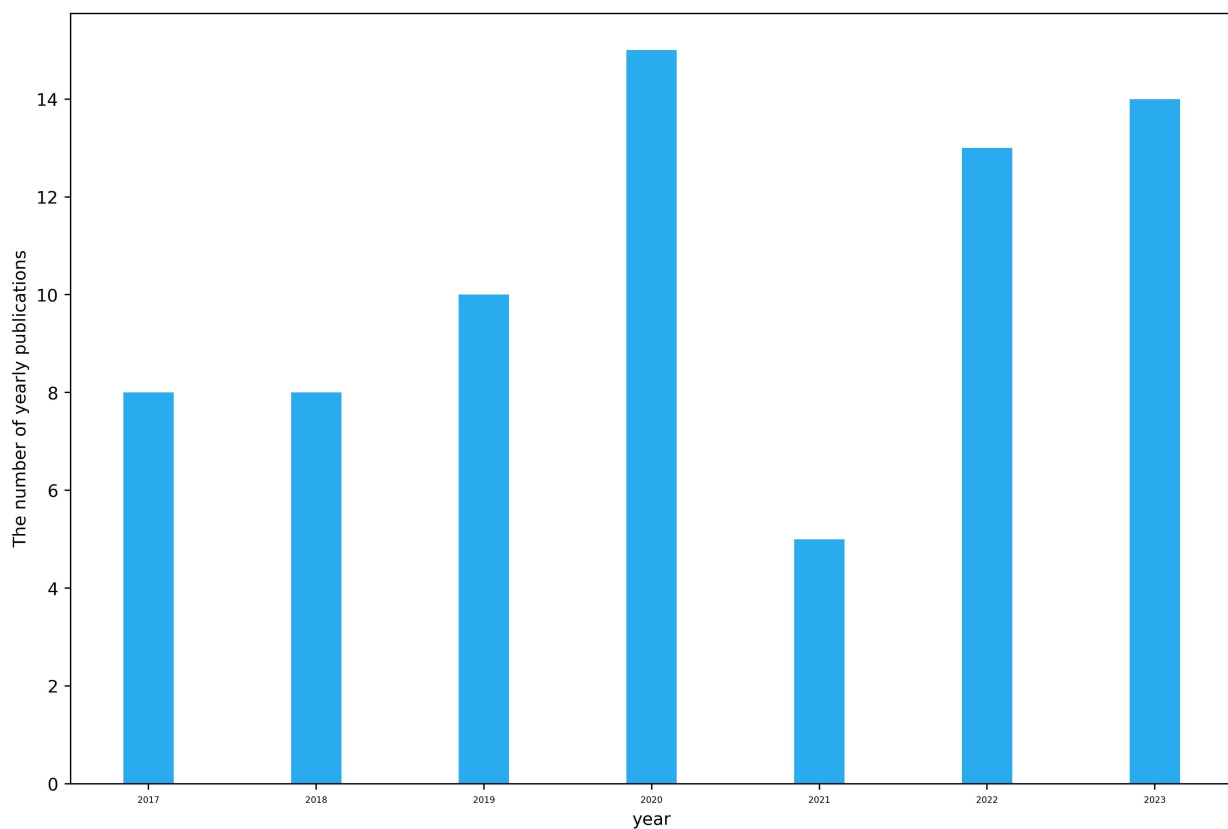


**Figure 3.** The number of yearly publications of LCCD.

The methods of land cover change detection typically involve using data from two or multiple periods. Figure 4 illustrates the process of change detection using satellite remote sensing data. We can observe that land cover change detection mainly consists of four parts: data preprocessing, change point detection, generation of land cover change maps, and result validation. The most critical part of the entire process is change point detection. Existing methods for land cover change point detection can be divided into post-classification comparison and direct comparison [54]. Post-classification comparison is a highly intuitive change detection method that is widely used. This method independently classifies remote sensing images in different phases and then compares and analyzes the results produced by classification. It can provide “from-to” change information. Additionally, the post-classification comparison method can overcome the problems caused by atmospheric conditions, sensors, seasons, and ground environment differences, further enhancing the precision of land cover change detection. The direct comparison method involves pixel-based and object-based. The pixel-based direct comparison method analyzes the pixels in the satellite remote sensing image to determine whether the pixels have changed. The object-based direct comparison method analyzes whether the object has

changed based on the object's geometric characteristics, shapes, textures, colors, and other attributes without classifying the images.

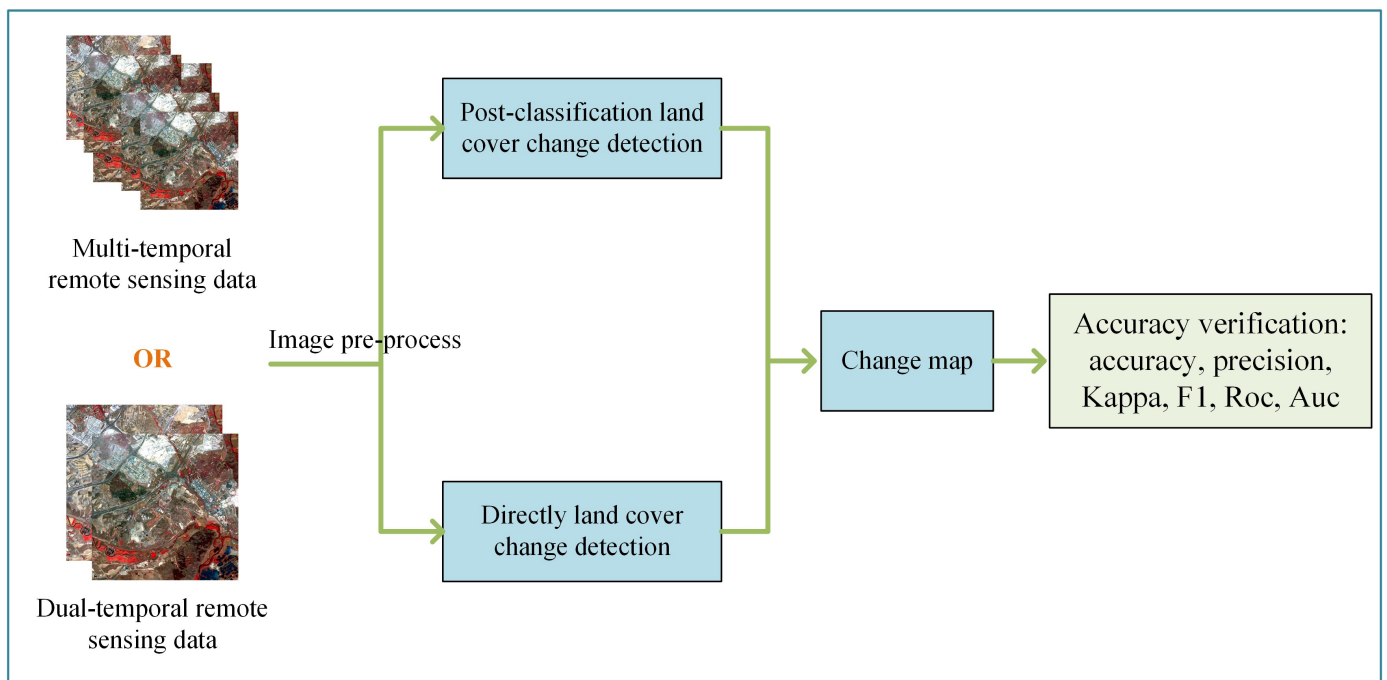


**Figure 4.** The process of change detection using satellite remote sensing data.

With the development of satellite technology and artificial intelligence, advanced methods of computer vision, including CNN, U-Net [55], GAN [56], Swin Transformer [57], SAM [58], and SegGpt [59], are utilized for land cover change detection. Consequently, numerous post-classification and direct comparison methods have been proposed for LCCD. These methods can be categorized into unsupervised, semi-supervised, and supervised learning, based on whether they use labeled samples and the number of labeled samples. Supervised learning requires a large number of labeled samples, semi-supervised methods can achieve good performance with fewer labeled samples, and unsupervised methods do not require any labeled samples. With sufficient training samples and prior knowledge, supervised methods can achieve higher accuracy. Additionally, these methods can be further divided into pixel-based and object-based approaches based on the analysis unit.

In the pixel-based method of LCCD, individual pixels serve as the analysis unit, and it provides better accuracy in analyzing changes in small-scale geographical objects compared to the object-based method. However, when pixels within the same geographical object are classified into different categories due to spectral variation, the original uniform object is “broken”, resulting in “salt and pepper noise”, leading to a decrease in accuracy [60]. On the other hand, the object-based method segments the remote sensing image into objects within a single area based on geometric characteristics, contextual relations, and spatial relations. It then detects changes in these objects over time. The object-based method effectively mitigates the influence of “salt and pepper noise” on LCCD and enhances detection accuracy [61–63]. Nonetheless, object-based methods are significantly influenced by mixed pixels, image resolution, land object scale, and segmentation methods. Figure 5 provides a detailed classification of existing methods, which will be reviewed in detail in the following sections.



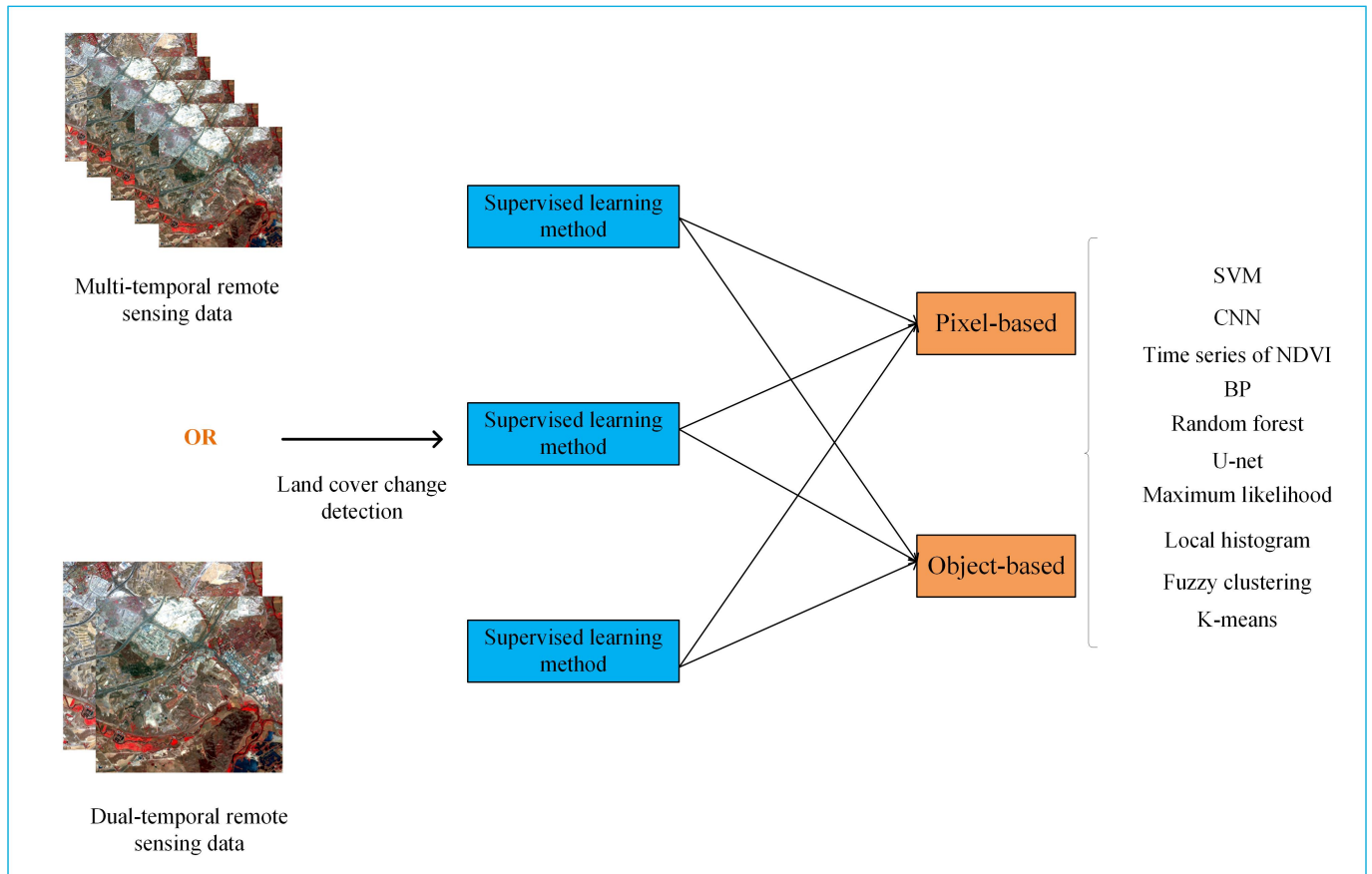


**Figure 5.** The detailed classification of existing methods.

### 3.1. Supervised Learning Method

Supervised learning methods for detecting land cover change require a large amount of labeled data and are widely utilized in the field of LCCD. Various algorithms have been proposed by researchers to address different challenges in this domain, and these methods are primarily categorized into two types: pixel-based and object-based approaches [64–69]. This section reviews and discusses in depth the existing methods of these two classes.

In the early stages, methods for LCCD relied on traditional machine learning techniques such as Maximum Likelihood [70–79], Support Vector Machine (SVM) [80], and Random Forest (RF) [81,82] for classifying land features, followed by vector change comparison to generate change maps. Fabian and Tikuye utilized satellite remote sensing data to train an RF model to classify land features into different types and subsequently analyzed the land cover change [81,82]. M.H. Elagouz employed an SVM for land type classification and then performed vectorization, calculation, and comparison of the classified data from different periods to obtain change maps [80]. These methods that perform change detection after classification can yield rich information about land cover changes. However, such methods require manual feature selection and processing. As deep learning has advanced, a multitude of land cover change detection techniques leveraging deep learning have emerged [83]. Seyd Teymoor utilized convolutional neural networks (CNN) to detect land cover changes and analyze the changes of rivers, farmland, and urban land [51]. Sangram Panigrahi employed a Focus Time-Delayed Neural Network (FTDNN) to detect land cover changes using time series data from specific locations [84].

To effectively utilize the spatiotemporal information present in satellite remote sensing images, Oliver Seifin combined Fully Convolutional Networks (FCN) and Long Short-Term Memory (LSTM) networks for land cover change detection [85]. Lichao Mou introduced the use of Recurrent Convolutional Neural Networks, combined with CNN and RNN, for detecting city expansion, grassland change, soil change, and water change [86]. Addition-

ally, Qiqi Zhu proposed a Siamese global learning framework to detect land cover changes, aimed at addressing the issues of few training samples and imbalanced samples [87].

To address the problem of inconsistent feature scales in LCCD, Yiqun Zhu proposed a fusion model based on self-attention networks and CNN, which can effectively capture multi-scale and local features to refine the results of LCCD [88]. Zhiyong Lv proposed a multi-scale network of LCCD guided by change gradient images, embedding multiscale information attention modules into the U-Net backbone network to merge multi-scale information from dual-date images [89].

In the context of the extensive application of transformer models in computer vision, Glenn R used TempCNN and transformer for LCCD [90]. Yaping Wu proposed a cross-attention mechanism to extract the feature differences between two-phase images based on a Swin Transformer [91].

Object-based methods have also gained prominence due to the presence of significant salt-and-pepper noise in acquired remote sensing images, which can affect the accuracy of pixel-based methods. Fangzhou Hong utilized a Fractal Net Evolution Approach (FNEA) to segment the remote sensing imagery and subsequently used a decision tree to classify the segmented objects and generate change maps [92]. Ran Jing combined a Multi-Scale Simple Linear Iterative Clustering Convolutional Neural Network (SLICCNN) with Stacked Convolutional Autoencoder (SCAE) features to enhance the change detection capability and optimized the change results using a Bayesian network [93].

Furthermore, Eduarda Martiniano de Oliveira Silveira proposed a novel land cover change detection method to eliminate the impact of phenology on change detection, employing a multi-resolution segmentation approach to create objects and an SVM algorithm for change detection classification [94]. Lei Ding used SAM to segment satellite remote sensing images and then employed an object-based change detection method to obtain land cover change maps. This represents the first introduction of the large visual segmentation model into land cover change detection, surpassing other segmentation models [95].

These recent advancements demonstrate the wide utilization of cutting-edge techniques such as deep learning, object-based methods, and transformer models in the domain of land cover change detection, each contributing to improved accuracy and efficiency.

### 3.2. Semi-Supervised Learning Method

Supervised LCCD methods typically require a significant amount of labeled data. However, annotating remote sensing image data is a challenging task, especially for large-scale remote sensing data. Therefore, researchers have proposed semi-supervised learning methods to address this issue. Syeda Maria Zaidi introduced a Semi-Supervised Image Classification (SSIC) based on maximum likelihood classification for land cover change detection [96]. Yangpeng Zhu presented a deep-learning framework that uses a sample augmentation algorithm based on the Pearson correlation coefficient for better performance on datasets with few samples [97]. Seyd Teymoor Seydi proposed a new supervised land cover change method by combining similarity-based and distance-based approaches, suitable for limited training samples and unaffected by noise and atmospheric conditions [98]. Zhiyong Lv introduced an Iterative Training Sample Augmentation (ITSA) strategy combined with deep learning neural networks to enhance the performance of the land cover change method [99].

To address the limitation of labeled data, Daifeng Peng proposed a novel semi-supervised convolutional network for CD (SemiCDNet) based on a generative adversarial network (GAN). This approach utilizes both labeled and unlabeled data to produce initial predictions and entropy maps, with two discriminators adopted to enforce feature distribution consistency for segmentation maps and entropy maps between the labeled and unlabeled data [100].

Considering the inherent shortcomings of the pixel-based method, Xiaokang Zhang proposed an object-based framework that combines deep feature learning (DFL) and a semi-supervised change vector (SCV) model for detecting changes in multi-temporal high-

resolution remote sensing images. This algorithm enhances the separability of change and unchanged objects without the need for any prior information [101]. These semi-supervised learning approaches represent important advancements in addressing the challenges of limited labeled data in LCCD.

### 3.3. Unsupervised Learning Method

Unsupervised learning methods for land cover detection do not require labeled data and are suitable for processing large-scale, difficult-to-label remote sensing image data. Early, pixel-based methods using satellite images for land cover change detection primarily included clustering, thresholding, and time series analysis.

Gabriela Ribeiro Sapucci combines Principal Component Analysis (PCA) and the K-means to detect land cover change [102]. Yafei Wang introduced a novel framework based on spatiotemporal fuzzy clustering, which enhances the accuracy by comparing the fuzzy similarity of time series curves for each pixel [103]. Tuomas Häme utilized a hierarchical clustering method for land cover change detection [104]. Daniela Espinoza-Molina uses the time series and K-means to detect change. This method uses vegetation and spectral indices to represent each image and extracts local features from these representations. Subsequently, K-means is employed to classify the extracted local features into different types. Finally, use the number of times each point changes to obtain land cover change information [105]. Yongguang Hu used an Iterative Self-Organizing (ISO) clustering method to quantify land cover changes [106].

Shwarnali Bhattacharjee employed the Normalized Difference Vegetation Index (NDVI) and thresholding for land cover classification and change detection [107]. Heena Kaldane used unsupervised Normalized Difference Ratio (NDR) as a change index (CI) and then applied thresholding to extract binary masks for changed and unchanged areas [108]. Boyu Liu proposed a change detection method based on multiple shape parameters using NDVI values and spectral values [109]. Cláudia M. Viana used 21 years of remote sensing image data to compute the time series of NDVI and NDWI. Then Time-Weighted Dynamic Time Warping (TWDTW) was used for time series classification, ultimately detecting pixels with land cover changes [110]. Yanghua Zhang generated time series for each pixel by extracting biophysical component indices (BCI) and NDVI from satellite images for land cover change detection [111]. Da He proposed an SST\_MAP model based on Joint Spectral-Spatial MAP (SST\_MAP) for observing scenes in remote sensing image time series to address low-resolution issues [112]. Jianshu Wang generated NDVI time series images of a study area over 12 months based on high spatiotemporal resolution PlanetScope satellite imagery for land cover change detection [113].

The method of cluster-based, time-series-based, and threshold-based play a crucial role in change detection on land cover. However, the accuracy of these methods is directly influenced by the reasonable setting of thresholds, clustering parameters, and noise. Therefore, Jining Yan proposed a Similarity Measurement-based Transfer Learning Time Series Adaptive Change Detection (SDTL-TSACD) model to detect land cover change [114]. Due the it is exist the speckle noise in SAR imagery, Wei Fang introduced a bi-objective fuzzy local information clustering method with decomposition to solve this issue. This method generates first-order difference images using the logarithmic mean ratio method and obtains second-order difference images using a combination of homomorphic filtering and saliency detection, effectively removing speckle noise [115]. Zhiyong Lv uses a Gaussian filter and an iterative optimization strategy to reduce noise and employs an improved region-growing algorithm to iteratively construct the final change detection map [116]. Zhiyong Lv designed a novel neural network with a spatial-spectral attention mechanism and a multi-scale dilated convolution module. This is used to address false changes and noise in change detection [26].

Additionally, to identify false changes, Zhiyong Lv proposed a method based on local histogram analysis to detect land cover changes, which suppresses false changes by adaptively defining local histogram trends. The local histogram trend analysis is used to measure

the magnitude of change between pixels, resulting in a land change magnitude image, which is then thresholded to obtain a binary land change map [117]. To mitigate the impact of phenology on land cover change detection, Zhiyong Lv proposed an Adaptive Histogram Trend (AHT) similarity method to quantitatively measure the size of corresponding pixels in bi-temporal images based on change semantics [118]. For different-scale features, F. Javier Cardama uses multiple detectors based on different segmentation algorithms to segment features of different scales and compute change maps by CVA-SAM [119]. Zhifeng Zheng introduced a new method for land cover change detection based on spatial-spectral feature fusion and multi-scale segmentation voting decisions [120]. Jin Xing proposed a scale-invariant change detection method for land cover change detection that avoids the distortion of LCCD caused by resampling [121]. Moreover, some methods utilize contextual information for land cover change recognition. Zhiyong Lv introduced a parameter-free land cover change detection method that uses an adaptive spatial context extraction algorithm to explore context information around pixels. It calculates the magnitude of change between paired pixels and employs a binary threshold method called double-window flexible pace search (DFPS) to create a Change Detection Map (CDM) [122,123].

With the development of deep learning, Nitesh Naik proposed the use of self-supervised learning to detect land changes. This method combines superpixel segmentation, difference image generation, feature extraction, clustering, deep learning classification, and image merging to achieve land cover change detection [124]. Chi Zhang introduced a fully Atrous convolutional neural network (FACNN) for land cover classification. A pixel-based change map is then generated based on the classification map of current images and an outdated land cover Geographic Information System (GIS) map [125]. Fei Song proposed a robust method for mountainous land cover change detection. This method generates multi-scale feature descriptions using a pre-trained VGG network and employs a Fuzzy C-Means classifier to generate a similarity matrix. The change map is then generated based on feature similarity [126]. Seyd Teymoor Seydi introduced a method based on a multi-dimensional deep Siamese network. Firstly, the training samples are automatically generated using the Otsu algorithm and Dynamic Time Warping (DTW) predictor and then obtain the binary change map by CNN [127].

Similarly, in unsupervised learning methods, numerous object-based land cover change detection methods have been proposed to reduce the impact of salt-and-pepper noise on land cover change detection. J.V.D. Prasad used a V-Net network to segment bi-temporal remote sensing images, dividing the original satellite remote sensing images into multiple objects. Then, a bilateral attention network is used to learn more discriminative features from the images. Finally, the features of the bi-temporal images are compared to obtain information about land cover changes [128]. Kaisheng Luo used Object-Based Image Analysis (OBIA) to segment objects into different regions and classify them. The land cover maps from the two different time periods are overlaid to generate the final land cover change map [129]. Jinxia Zhu proposed an automated object-based multi-source change detection method using a Gaussian Mixture Model to detect land cover changes [130]. Zhihao Wang introduced a method with dual-constrained thresholds for change intensity and Object-Level Correlation Coefficient (ODCD). This aims to reduce feature dimensionality and improve computational efficiency, objectivity, and accuracy. The Change Vector Analysis (CVA) method is used to generate a change magnitude map, which is then thresholded to produce a land cover change map [131]. Sunan Shi proposed a Class-Prioritized Conditional Random Field (COCRF) framework for land cover change detection. It reduces the impact of spectral variability [132]. Donato Amitrano introduced an unsupervised land cover change detection method by using object-based image analysis of multi-temporal geographical objects [133]. To mitigate the influence of false changes on land cover change detection, Zhiyong Lv proposed an Object-Oriented Key Point Vector Distance (KPVD) to measure the change magnitude and then use a thresholding method to divide the change magnitude image into a binary change detection map [134].

Object-based land cover change detection is a crucial aspect of remote sensing. However, these approaches ignore the fact that objects may only change partially, resulting in uncertain classification information. To reduce this uncertainty, Tong Xiao proposed an improved Rough Fuzzy Possibilistic C-Means Clustering Method (MRFPCM) that combines multi-resolution scale information. MRFPCM classifies the segmented objects layer by layer until there are no uncertain objects left [135].

### 3.4. Evaluation Metrics

The typical evaluation metrics used to evaluate the performance of LCCD methods include accuracy, F1-Score, sensitivity, specificity, receiver operating characteristic (ROC) curve, and kappa coefficient (Kappa). This section describes these general evaluation metrics.

#### 3.4.1. Accuracy

Accuracy is the most common and simple evaluate metric of classification, which is easy to calculate and intuitive to understand. The calculation formula is as follows [136]:

$$Accuracy = \frac{TP + TN}{TP + FP + TN + FN} \quad (1)$$

where  $TN$  and  $FN$  represent the true negatives and false negatives,  $TP$  and  $FP$  denotes the true positives and false positives, respectively.

#### 3.4.2. F1-Score

F1-Score is a metric used to measure the performance of the classification model. In the context of imbalanced datasets, the accuracy is not a robust measurement, F1-Score is a more credible metric to evaluate the performance of LCCD. The specific calculation formula is as follows [136]:

$$F1-Score = 2 \times \frac{Precision \times Recall}{Precision + Recall} \quad (2)$$

where  $Precision = \frac{TP}{TP+FP}$  and  $Recall = \frac{TP}{TP+TN}$

#### 3.4.3. Sensitivity and Specificity

Specificity and sensitivity are two important metrics used to evaluate the performance of a binary classification model, which is Widely used in land cover change detection. The calculation formulas for these two metrics are as follows [137]:

$$Sensitivity = \frac{TP}{TP + FN} \quad (3)$$

$$Specificity = \frac{TN}{TN + FP} \quad (4)$$

#### 3.4.4. ROC

The ROC curve provides a comprehensive evaluation of the performance of the classification model under different thresholds. By observing the points on the curve, we can understand the trade-off between sensitivity and specificity of the model [136].

#### 3.4.5. Kappa Coefficient

Cohen's Kappa is a statistical index used to measure the consistency of classification models. It is used to evaluate the consistency between two or more observers or the consistency of LCCD methods [138]. The definition of  $k$  is:

$$k = \frac{p_0 - p_e}{1 - p_e} = 1 - \frac{1 - p_0}{1 - p_e} \quad (5)$$

where where  $p_e$  represents the hypothetical probability of chance agreement and  $p_0$  denotes the relative observed agreement among raters, respectively.

#### 4. Discussion

Despite the considerable progress in AI technology and satellite remote sensing for LCCD, the method based on satellite remote sensing data still encounters limitations compared to traditional LCCD methods. Additionally, unresolved challenges persist in utilizing AI technology and satellite remote sensing for LCCD. This section primarily focuses on the limitations of using satellite remote sensing images and examines the challenges and future directions of integrating AI technology and satellite remote sensing for LCCD.

##### 4.1. Limitations of Satellite Remote Sensing

Satellite remote sensing offers significant advantages, such as lower cost, wide coverage, and long observation periods, making it a valuable resource for LCCD. Nevertheless, it presents certain limitations. The spatial and temporal resolution, susceptibility to cloud cover and atmospheric conditions, constraints in spectral and radiometric resolution, potential errors in interpretation and classification, limitations in data availability and cost, as well as complexities in data processing and analysis highlight the challenges involved in leveraging satellite remote sensing for LCCD. Rigorous approaches to data selection, processing techniques, and validation methods are necessary to ensure dependable and precise outcomes.

##### 4.2. Challenges and Future Prospects of LCCD

LCCD is one of the key applications in remote sensing image analysis, helping monitor changes in land use, urban expansion, natural disasters, and more. In Section 3, we categorize land cover detection methods based on the use of labeled data, dividing them into supervised learning, semi-supervised learning, and unsupervised learning approaches. Supervised learning methods can achieve high detection accuracy when there is sufficient labeled data, but acquiring and maintaining labeled data can be costly. Semi-supervised learning methods leverage a small amount of labeled data in combination with unlabeled data to improve detection accuracy. Unsupervised learning methods automatically detect differences in images without the need for labeled data, making them suitable for large-scale LCCD tasks. All three methods can yield good results in practical applications, but challenges persist in the field of LCCD.

###### 4.2.1. Explainable AI (XAI)

Although data-driven techniques, especially deep learning (DL) models and large models, have achieved state-of-the-art results in LCCD, their black-box operations impede the comprehension of their decision-making, hindering the identification of biases and limitations in LCCD methods' performance [139]. Furthermore, the lack of explanations in DL models regarding the influence of feature samples on model performance and the rationale behind predictions [140] accentuates the need for explainable artificial intelligence (XAI) to facilitate practical deployments of AI technology for LCCD.

The purpose of an XAI system is to make its behavior more intelligible to humans by providing explanations. There are some general principles to help create effective, more human-understandable AI systems: The XAI system should be able to explain its capabilities and understandings; explain what it has done, what it is doing now, and what will happen next; and disclose the salient information that it is acting on. However, every explanation is set within a context that depends on the task, abilities, and expectations of the user of the AI system. The definitions of interpretability and explainability are, thus, domain dependent and may not be defined independently from a domain.

#### 4.2.2. The Noise of Satellite Remote Sensing

The noise issue in satellite remote sensing images significantly affects the performance of LCCD methods. However, current approaches mainly focus on addressing salt-and-pepper noise and speckle noise while somewhat neglecting the impact of other types of noise on detection results. To address this challenge, more advanced filtering techniques like wavelet transforms, mean-shift, non-local means, and others can be employed to mitigate the adverse effects of various noise types. Furthermore, extensive sample data and training can help algorithms better adapt to noise, thereby enhancing robustness against different types of noise.

#### 4.2.3. Real-Time Detection of Land Cover Change

Currently, there are relatively few methods for real-time detection of land cover change, and these methods often struggle to capture the potential impact of phenological changes on detection results. Phenological factors such as seasonal variations, weather conditions, and vegetation growth cycles can cause changes in the brightness, color, and texture of remote sensing images, thereby complicating land cover change detection. This challenge is particularly significant in applications related to environmental monitoring, resource management, and natural disaster monitoring. To address this challenge, the following approaches can be employed: (1) Integration of Multiple Data Sources: Integrate various data sources, including multispectral and hyperspectral imagery, meteorological data, soil data, and more, to gain a comprehensive understanding of surface feature changes under different seasons and weather conditions. This helps in more accurately distinguishing phenological changes from genuine land cover changes. (2) Utilization of Phenological Data: Utilize phenological data such as vegetation indices and land surface temperature to aid in distinguishing natural changes from anthropogenic changes. These data can be used to develop more refined land cover change detection algorithms.

#### 4.2.4. Multi-Resolution Remote Sensing Image Fusion

High-resolution images provide richer surface details, allowing them to capture small-scale land cover changes such as buildings, roads, vegetation, and more. This enables more accurate detection and differentiation of various land cover types, particularly beneficial in applications like urban planning and environmental monitoring. The advantage of high-resolution images lies in their ability to capture minute changes, such as building expansions or tree removal. However, high-resolution images typically generate a large amount of data, requiring more computational resources for processing and storage. Additionally, high-resolution image acquisition frequencies are often lower, making them less suitable for applications that require frequent monitoring. Moreover, collecting and purchasing high-resolution images can incur higher costs. In contrast, low-resolution images are suitable for global-scale land cover change monitoring across extensive geographic areas. They usually have higher acquisition frequencies, making them suitable for applications that require frequent monitoring, such as meteorology and agriculture. Furthermore, low-resolution images are typically more cost-effective, with lower data acquisition costs. However, low-resolution images may lose some surface details and may not capture small-scale land cover changes. For certain land cover types, such as different types of vegetation or buildings, low-resolution images may not provide sufficient differentiation. Therefore, effectively fusing multi-resolution remote sensing image may improve the performance of LCCD methods in the future.

#### 4.2.5. Detect the Multi-Scale Geographic Object Change

The scale of different land cover features varies, with some occupying several pixels in remote sensing images, while others are contained within a single pixel, either individually or as a mix of different features. This leads to difficulties in distinguishing land cover boundaries. Detecting land cover changes for different-scale features is a challenge. To address this issue, the post-processing techniques such as boundary smoothing and region

merging can be applied to improve the distinction of land features. This can help reduce problems caused by inconsistent scales. Alternatively, the method of fusing remote sensing data of different resolutions can be employed to obtain more comprehensive and accurate information. This fusion can include merging high-resolution images with low-resolution images or using multiple resolution levels of images. Fusion techniques can involve pixel-level fusion, feature-level fusion, and data fusion to enhance feature recognition and discrimination. Additionally, with the development of visual segmentation large language models (LLM) such as SAM, SEEM, and SegGpt, they can further be used for LCCD.

#### 4.2.6. Point Clouds for LCCD

Point clouds are considered one of the principal pillars for 3D digital world representation, capturing the elevation and shape of ground objects more comprehensively than traditional two-dimensional images. The development of sensors for acquiring point cloud information for scalable and flexible geometric representations has introduced new ideas, technologies, and solutions for improving the LCCD method [141].

Some studies have utilized point cloud data in land cover and land use classification. Salah proposed a point-clouds-based approach to detect LULC changes from light detection and ranging (LiDAR) images, where point-cloud data was extracted from stereo satellite imagery [142]. Tseng introduced a Waveform-based classifier for clarifying and classifying point clouds of LULCs [143]. Furthermore, Zhou proposed a CNN-based LULC classification method, integrating point cloud data and very high spatial resolution satellite remote sensing imagery for LULC [144].

Additionally, point cloud data can provide higher spatial resolution, enabling more accurate detection of small-scale ground objects or microscopic changes. Thus, in the future, combining point cloud data with satellite remote sensing may enhance the accuracy of LCCD methods.

## 5. Conclusions

LCCD is crucial in natural disaster monitoring, agricultural yield assessment, deforestation tracking, and ecological environment evaluation. With the continuous advancement of satellite remote sensing technology, acquiring multi-temporal ground observation data has become increasingly accessible, leading to the development of numerous LCCD methods based on satellite remote sensing data. Therefore, our aim is to comprehensively review these methods using artificial intelligence (AI) and satellite remote sensing, specifically focusing on the most advanced AI technology applied in LCCD, by analyzing relevant literature published after 2017. We categorize existing methods into supervised, semi-supervised, and unsupervised approaches based on whether they require labeled data. Furthermore, we classify the methods of LCCD into pixel-based and object-based methods, providing a detailed literature analysis. Through this examination, we aim to identify the challenges that current change detection techniques still face in terms of data, models, and application domains, and propose potential solutions to address these challenges. The content of this article aims to assist researchers and practitioners in this field by providing insights into current trends, the latest technologies, and methodological approaches, aiding them in choosing appropriate research directions and driving further advancements in the field of LCCD.

Moreover, the development of robust and powerful LCCD methods is strongly influenced by the quality of the AI models deployed and the availability of remote sensing data used for their training. However, the validation of most existing frameworks using private datasets presents challenges in informing the state-of-the-art and conducting fair comparisons. The introduction of explainable AI is significant as it helps humans understand the results generated by AI models, departing from the “black-box” concept. Additionally, fully understanding image regions using the idea of point clouds remains challenging, encompassing point cloud registration and fusion, semantic labeling, feature extraction, segmentation, and classification. Finally, the introduction of more advanced AI-based



fusion for improving spatial resolution, the capabilities of feature displays, and geometric precision plays a significant role in enhancing LCCD accuracy.

**Author Contributions:** Writing—Original Draft Preparation, Z.G. and M.Z.; Writing—Review and Editing, Supervision, Z.G. and M.Z. All authors have read and agreed to the published version of the manuscript.

**Funding:** This research was funded by National Natural Science Foundation of China (grant number 32371966).

**Data Availability Statement:** Not applicable.

**Conflicts of Interest:** The authors declare no conflict of interest.

## References

1. Wang, Y.; Sun, Y.; Cao, X.; Wang, Y.; Zhang, W.; Cheng, X. A Review of Regional and Global Scale Land Use/Land Cover (LULC) Mapping Products Generated from Satellite Remote Sensing. *ISPRS J. Photogramm. Remote Sens.* **2023**, *206*, 311–334. [[CrossRef](#)]
2. Geist, H.J.; Lambin, E.F. Proximate causes and underlying driving forces of tropical deforestation: Tropical forests are disappearing as the result of many pressures, both local and regional, acting in various combinations in different geographical locations. *BioScience* **2002**, *52*, 143–150. [[CrossRef](#)]
3. Lakshumanan, C.; Kishore, Y.P.; Yiveganandan, S.; Krishnakumar, P.; Muthusankar, G. Landuse/land cover dynamics study in Nilgiris district part of Western Ghats, Tamilnadu. *Int. J. Geomat. Geosci.* **2012**, *2*, 911–923.
4. Dubovyk, O. The role of Remote Sensing in land degradation assessments: Opportunities and challenges. *Eur. J. Remote Sens.* **2017**, *50*, 601–613. [[CrossRef](#)]
5. Pawe, C.K.; Saikia, A. Unplanned urban growth: Land use/land cover change in the Guwahati Metropolitan Area, India. *Geogr. Tidsskr.-Dan. J. Geogr.* **2018**, *118*, 88–100. [[CrossRef](#)]
6. Deka, J.; Tripathi, O.P.; Khan, M.L.; Srivastava, V.K. Study on land-use and land-cover change dynamics in Eastern Arunachal Pradesh, NE India using remote sensing and GIS. *Trop. Ecol.* **2019**, *60*, 199–208. [[CrossRef](#)]
7. Gessesse, B.; Bewket, W. Drivers and implications of land use and land cover change in the central highlands of Ethiopia: Evidence from remote sensing and socio-demographic data integration. *Ethiop. J. Soc. Sci. Humanit.* **2014**, *10*, 1–23.
8. Fentie, S.F.; Jembere, K.; Fekadu, E.; Wasie, D. Land use and land cover dynamics and properties of soils under different land uses in the tejibara watershed, Ethiopia. *Sci. World J.* **2020**, *2020*, 1479460. [[CrossRef](#)]
9. Khan, I.; Javed, T.; Khan, A.; Lei, H.; Muhammad, I.; Ali, I.; Huo, X. Impact assessment of land use change on surface temperature and agricultural productivity in Peshawar-Pakistan. *Environ. Sci. Pollut. Res.* **2019**, *26*, 33076–33085. [[CrossRef](#)]
10. Ali, A.; Khalid, A.; Butt, M.A.; Mehmood, R.; Mahmood, S.A.; Sami, J.; Qureshi, J.; Shafique, K.; Ghalib, A.K.; Waheed, R.; et al. Towards a remote sensing and GIS-based technique to study population and urban growth: A case study of Multan. *Adv. Remote Sens.* **2018**, *7*, 245–258. [[CrossRef](#)]
11. Khan, S.H.; He, X.; Porikli, F.; Bennamoun, M. Forest change detection in incomplete satellite images with deep neural networks. *IEEE Trans. Geosci. Remote Sens.* **2017**, *55*, 5407–5423. [[CrossRef](#)]
12. Chen, X.L.; Zhao, H.M.; Li, P.X.; Yin, Z.Y. Remote sensing image-based analysis of the relationship between urban heat island and land use/cover changes. *Remote Sens. Environ.* **2006**, *104*, 133–146. [[CrossRef](#)]
13. Ghorbanzadeh, O.; Blaschke, T.; Gholamnia, K.; Meena, S.R.; Tiede, D.; Aryal, J. Evaluation of different machine learning methods and deep-learning convolutional neural networks for landslide detection. *Remote Sens.* **2019**, *11*, 196. [[CrossRef](#)]
14. Radke, R.J.; Andra, S.; Al-Kofahi, O.; Roysam, B. Image change detection algorithms: A systematic survey. *IEEE Trans. Image Process.* **2005**, *14*, 294–307. [[CrossRef](#)] [[PubMed](#)]
15. Mahdavi, S.; Salehi, B.; Huang, W.; Amani, M.; Brisco, B. A PolSAR change detection index based on neighborhood information for flood mapping. *Remote Sens.* **2019**, *11*, 1854. [[CrossRef](#)]
16. Hoque, M.A.A.; Phinn, S.; Roelfsema, C.; Childs, I. Tropical cyclone disaster management using remote sensing and spatial analysis: A review. *Int. J. Disaster Risk Reduct.* **2017**, *22*, 345–354. [[CrossRef](#)]
17. Anniballe, R.; Noto, F.; Scalia, T.; Bignami, C.; Stramondo, S.; Chini, M.; Pierdicca, N. Earthquake damage mapping: An overall assessment of ground surveys and VHR image change detection after L'Aquila 2009 earthquake. *Remote Sens. Environ.* **2018**, *210*, 166–178. [[CrossRef](#)]
18. Li, Z.; Shi, W.; Myint, S.W.; Lu, P.; Wang, Q. Semi-automated landslide inventory mapping from bitemporal aerial photographs using change detection and level set method. *Remote Sens. Environ.* **2016**, *175*, 215–230. [[CrossRef](#)]
19. Li, Z.; Shi, W.; Lu, P.; Yan, L.; Wang, Q.; Miao, Z. Landslide mapping from aerial photographs using change detection-based Markov random field. *Remote Sens. Environ.* **2016**, *187*, 76–90. [[CrossRef](#)]
20. Wu, Y.; Ding, H.; Gong, M.; Qin, A.; Ma, W.; Miao, Q.; Tan, K.C. Evolutionary multiform optimization with two-stage bidirectional knowledge transfer strategy for point cloud registration. *IEEE Trans. Evol. Comput.* **2022**. [[CrossRef](#)]
21. Liu, S.; Zheng, Y.; Dalponte, M.; Tong, X. A novel fire index-based burned area change detection approach using Landsat-8 OLI data. *Eur. J. Remote Sens.* **2020**, *53*, 104–112. [[CrossRef](#)]

22. Leichtle, T. Change Detection for Application in Urban Geography Based on Very High Resolution Remote Sensing. 2020. Available online: <https://edoc.hu-berlin.de/handle/18452/21797> (accessed on 6 November 2023).
23. Wang, N.; Li, W.; Tao, R.; Du, Q. Graph-based block-level urban change detection using Sentinel-2 time series. *Remote Sens. Environ.* **2022**, *274*, 112993. [[CrossRef](#)]
24. Ban, Y.; Yousif, O.A. Multitemporal spaceborne SAR data for urban change detection in China. *IEEE J. Sel. Top. Appl. Earth Obs. Remote Sens.* **2012**, *5*, 1087–1094. [[CrossRef](#)]
25. Lv, Z.; Wang, F.; Cui, G.; Benediktsson, J.A.; Lei, T.; Sun, W. Spatial–spectral attention network guided with change magnitude image for land cover change detection using remote sensing images. *IEEE Trans. Geosci. Remote Sens.* **2022**, *60*, 1–12. [[CrossRef](#)]
26. Song, K.; Jiang, J. AGCDetNet: An attention-guided network for building change detection in high-resolution remote sensing images. *IEEE J. Sel. Top. Appl. Earth Obs. Remote Sens.* **2021**, *14*, 4816–4831. [[CrossRef](#)]
27. Bhatta, B.; Saraswati, S.; Bandyopadhyay, D. Urban sprawl measurement from remote sensing data. *Appl. Geogr.* **2010**, *30*, 731–740. [[CrossRef](#)]
28. Hegazy, I.R.; Kaloop, M.R. Monitoring urban growth and land use change detection with GIS and remote sensing techniques in Daqahlia governorate Egypt. *Int. J. Sustain. Built Environ.* **2015**, *4*, 117–124. [[CrossRef](#)]
29. Gao, J.; Liu, Y. Determination of land degradation causes in Tongyu County, Northeast China via land cover change detection. *Int. J. Appl. Earth Obs. Geoinf.* **2010**, *12*, 9–16. [[CrossRef](#)]
30. Taubenböck, H.; Esch, T.; Felbier, A.; Wiesner, M.; Roth, A.; Dech, S. Monitoring urbanization in mega cities from space. *Remote Sens. Environ.* **2012**, *117*, 162–176. [[CrossRef](#)]
31. Zhang, T.; Huang, X. Monitoring of urban impervious surfaces using time series of high-resolution remote sensing images in rapidly urbanized areas: A case study of Shenzhen. *IEEE J. Sel. Top. Appl. Earth Obs. Remote Sens.* **2018**, *11*, 2692–2708. [[CrossRef](#)]
32. White, J.C.; Coops, N.C.; Wulder, M.A.; Vastaranta, M.; Hilker, T.; Tompalski, P. Remote sensing technologies for enhancing forest inventories: A review. *Can. J. Remote Sens.* **2016**, *42*, 619–641. [[CrossRef](#)]
33. Munyati, C. Wetland change detection on the Kafue Flats, Zambia, by classification of a multitemporal remote sensing image dataset. *Int. J. Remote Sens.* **2000**, *21*, 1787–1806. [[CrossRef](#)]
34. Xian, G.; Homer, C.; Fry, J. Updating the 2001 National Land Cover Database land cover classification to 2006 by using Landsat imagery change detection methods. *Remote Sens. Environ.* **2009**, *113*, 1133–1147. [[CrossRef](#)]
35. Gulhane, V.A.; Rode, S.V.; Pande, C.B. Correlation analysis of soil nutrients and prediction model through ISO cluster unsupervised classification with multispectral data. *Multimed. Tools Appl.* **2023**, *82*, 2165–2184. [[CrossRef](#)]
36. Awad, M.M. An innovative intelligent system based on remote sensing and mathematical models for improving crop yield estimation. *Inf. Process. Agric.* **2019**, *6*, 316–325. [[CrossRef](#)]
37. Cook-Patton, S.C.; Drever, C.R.; Griscom, B.W.; Hamrick, K.; Hardman, H.; Kroeger, T.; Pacheco, P.; Raghav, S.; Stevenson, M.; Webb, C.; et al. Protect, manage and then restore lands for climate mitigation. *Nat. Clim. Chang.* **2021**, *11*, 1027–1034. [[CrossRef](#)]
38. Baker, C.; Lawrence, R.L.; Montagne, C.; Patten, D. Change detection of wetland ecosystems using Landsat imagery and change vector analysis. *Wetlands* **2007**, *27*, 610–619. [[CrossRef](#)]
39. Bouziani, M.; Goïta, K.; He, D.C. Automatic change detection of buildings in urban environment from very high spatial resolution images using existing geodatabase and prior knowledge. *ISPRS J. Photogramm. Remote Sens.* **2010**, *65*, 143–153. [[CrossRef](#)]
40. Leichtle, T.; Geiß, C.; Wurm, M.; Lakes, T.; Taubenböck, H. Unsupervised change detection in VHR remote sensing imagery—An object-based clustering approach in a dynamic urban environment. *Int. J. Appl. Earth Obs. Geoinf.* **2017**, *54*, 15–27. [[CrossRef](#)]
41. Coppin, P.; Jonckheere, I.; Nackaerts, K.; Muys, B.; Lambin, E. Review Article Digital change detection methods in ecosystem monitoring: A review. *Int. J. Remote Sens.* **2004**, *25*, 1565–1596. [[CrossRef](#)]
42. Hussain, M.; Chen, D.; Cheng, A.; Wei, H.; Stanley, D. Change detection from remotely sensed images: From pixel-based to object-based approaches. *ISPRS J. Photogramm. Remote Sens.* **2013**, *80*, 91–106. [[CrossRef](#)]
43. Chen, G.; Hay, G.J.; Carvalho, L.M.; Wulder, M.A. Object-based change detection. *Int. J. Remote Sens.* **2012**, *33*, 4434–4457. [[CrossRef](#)]
44. Singh, P.; Kikon, N.; Verma, P. Impact of land use change and urbanization on urban heat island in Lucknow city, Central India. A remote sensing based estimate. *Sustain. Cities Soc.* **2017**, *32*, 100–114. [[CrossRef](#)]
45. Afaq, Y.; Manocha, A. Analysis on change detection techniques for remote sensing applications: A review. *Ecol. Inform.* **2021**, *63*, 101310. [[CrossRef](#)]
46. Asokan, A.; Anitha, J. Change detection techniques for remote sensing applications: A survey. *Earth Sci. Inform.* **2019**, *12*, 143–160. [[CrossRef](#)]
47. Lv, Z.; Liu, T.; Benediktsson, J.A.; Falco, N. Land cover change detection techniques: Very-high-resolution optical images: A review. *IEEE Geosci. Remote Sens. Mag.* **2021**, *10*, 44–63. [[CrossRef](#)]
48. MohanRajan, S.N.; Loganathan, A.; Manoharan, P. Survey on Land Use/Land Cover (LU/LC) change analysis in remote sensing and GIS environment: Techniques and Challenges. *Environ. Sci. Pollut. Res.* **2020**, *27*, 29900–29926. [[CrossRef](#)]
49. Wang, J.; Bretz, M.; Dewan, M.A.A.; Delavar, M.A. Machine learning in modelling land-use and land cover-change (LULCC): Current status, challenges and prospects. *Sci. Total Environ.* **2022**, *822*, 153559. [[CrossRef](#)]
50. Cheng, G.; Huang, Y.; Li, X.; Lyu, S.; Xu, Z.; Zhao, Q.; Xiang, S. Change Detection Methods for Remote Sensing in the Last Decade: A Comprehensive Review. *arXiv* **2023**, arXiv:2305.05813.

51. Seydi, S.T.; Hasanlou, M.; Amani, M. A new end-to-end multi-dimensional CNN framework for land cover/land use change detection in multi-source remote sensing datasets. *Remote Sens.* **2020**, *12*, 2010. [[CrossRef](#)]
52. Liu, S.; Bruzzone, L.; Bovolo, F.; Du, P. Hierarchical unsupervised change detection in multitemporal hyperspectral images. *IEEE Trans. Geosci. Remote Sens.* **2014**, *53*, 244–260.
53. Wu, C.; Du, B.; Zhang, L. A subspace-based change detection method for hyperspectral images. *IEEE J. Sel. Top. Appl. Earth Obs. Remote Sens.* **2013**, *6*, 815–830. [[CrossRef](#)]
54. Singh, A. Review article digital change detection techniques using remotely-sensed data. *Int. J. Remote Sens.* **1989**, *10*, 989–1003. [[CrossRef](#)]
55. Ronneberger, O.; Fischer, P.; Brox, T. U-net: Convolutional networks for biomedical image segmentation. In *Medical Image Computing and Computer-Assisted Intervention—MICCAI 2015, Proceedings of the International Conference on Medical Image Computing and Computer-Assisted Intervention, Munich, Germany, 5–9 October 2015*; Part III 18; Springer: Cham, Switzerland, 2015; pp. 234–241.
56. Goodfellow, I.; Pouget-Abadie, J.; Mirza, M.; Xu, B.; Warde-Farley, D.; Ozair, S.; Courville, A.; Bengio, Y. Generative adversarial nets. In *Advances in Neural Information Processing Systems 27, Proceedings of the NIPS 2014, Montreal, QC, Canada, 8–13 December 2014*; Curran: Red Hook, NY, USA, 2007.
57. Liu, Z.; Lin, Y.; Cao, Y.; Hu, H.; Wei, Y.; Zhang, Z.; Lin, S.; Guo, B. Swin transformer: Hierarchical vision transformer using shifted windows. In *Proceedings of the IEEE/CVF International Conference on Computer Vision, Montreal, BC, Canada, 11–17 October 2021*; pp. 10012–10022.
58. Zhang, C.; Han, D.; Qiao, Y.; Kim, J.U.; Bae, S.H.; Lee, S.; Hong, C.S. Faster Segment Anything: Towards Lightweight SAM for Mobile Applications. *arXiv* **2023**, arXiv:2306.14289.
59. Wang, X.; Zhang, X.; Cao, Y.; Wang, W.; Shen, C.; Huang, T. Seggpt: Segmenting everything in context. *arXiv* **2023**, arXiv:2304.03284.
60. Blaschke, T. Object based image analysis for remote sensing. *ISPRS J. Photogramm. Remote Sens.* **2010**, *65*, 2–16. [[CrossRef](#)]
61. Burnett, C.; Blaschke, T. A multi-scale segmentation/object relationship modelling methodology for landscape analysis. *Ecol. Model.* **2003**, *168*, 233–249. [[CrossRef](#)]
62. Benz, U.C.; Hofmann, P.; Willhauck, G.; Lingenfelder, I.; Heynen, M. Multi-resolution, object-oriented fuzzy analysis of remote sensing data for GIS-ready information. *ISPRS J. Photogramm. Remote Sens.* **2004**, *58*, 239–258. [[CrossRef](#)]
63. Zhang, X.; Du, L.; Tan, S.; Wu, F.; Zhu, L.; Zeng, Y.; Wu, B. Land use and land cover mapping using RapidEye imagery based on a novel band attention deep learning method in the three gorges reservoir area. *Remote Sens.* **2021**, *13*, 1225. [[CrossRef](#)]
64. Gomroki, M.; Hasanlou, M.; Reinartz, P. STCD-EffV2T Unet: Semi Transfer Learning EfficientNetV2 T-Unet Network for Urban/Land Cover Change Detection Using Sentinel-2 Satellite Images. *Remote Sens.* **2023**, *15*, 1232. [[CrossRef](#)]
65. Duveiller, G.; Defourny, P. A conceptual framework to define the spatial resolution requirements for agricultural monitoring using remote sensing. *Remote Sens. Environ.* **2010**, *114*, 2637–2650. [[CrossRef](#)]
66. Liu, Q.; Meng, X.; Li, X.; Shao, F. Detail Injection-Based Spatio-Temporal Fusion for Remote Sensing Images with Land Cover Changes. *IEEE Trans. Geosci. Remote Sens.* **2023**, *61*, 5401514. [[CrossRef](#)]
67. Wu, K.; Zhong, Y.; Wang, X.; Sun, W. A novel approach to subpixel land-cover change detection based on a supervised back-propagation neural network for remotely sensed images with different resolutions. *IEEE Geosci. Remote Sens. Lett.* **2017**, *14*, 1750–1754. [[CrossRef](#)]
68. Song, F.; Zhang, S.; Lei, T.; Song, Y.; Peng, Z. MSTDSNet-CD: Multiscale swin transformer and deeply supervised network for change detection of the fast-growing urban regions. *IEEE Geosci. Remote Sens. Lett.* **2022**, *19*, 6508505. [[CrossRef](#)]
69. Yang, S.; Song, F.; Jeon, G.; Sun, R. Scene Changes Understanding Framework Based on Graph Convolutional Networks and Swin Transformer Blocks for Monitoring LCLU Using High-Resolution Remote Sensing Images. *Remote Sens.* **2022**, *14*, 3709. [[CrossRef](#)]
70. Weslati, O.; Bouaziz, S.; Serbaji, M.M. Mapping and monitoring land use and land cover changes in Mellegue watershed using remote sensing and GIS. *Arab. J. Geosci.* **2020**, *13*, 687. [[CrossRef](#)]
71. Hlotov, V.; Biala, M. Spatial-temporal geodynamics monitoring of land use and land cover changes in Stebnyk, Ukraine based on Earth remote sensing data. *Geodynamics* **2022**, *1*, 5–15. [[CrossRef](#)]
72. Khan, A.R.; Khan, A.; Masud, S.; Rahman, R.M. Analyzing the Land Cover Change and Degradation in Sundarbans Mangrove Forest Using Machine Learning and Remote Sensing Technique. In *Advances in Computational Intelligence, Proceedings of the 16th International Work-Conference on Artificial Neural Networks, IWANN 2021, Virtual Event, 16–18 June 2021*; Part II 16; Springer: Cham, Switzerland, 2021; pp. 429–438.
73. Mugo, R.; Waswa, R.; Nyaga, J.W.; Ndubi, A.; Adams, E.C.; Flores-Anderson, A.I. Quantifying land use land cover changes in the Lake Victoria basin using satellite remote sensing: The trends and drivers between 1985 and 2014. *Remote Sens.* **2020**, *12*, 2829. [[CrossRef](#)]
74. Juliev, M.; Pulatov, A.; Fuchs, S.; Hübl, J. Analysis of Land Use Land Cover Change Detection of Bostanlik District, Uzbekistan. *Pol. J. Environ. Stud.* **2019**, *28*. [[CrossRef](#)]
75. Twisa, S.; Buchroithner, M.F. Land-use and land-cover (LULC) change detection in Wami River Basin, Tanzania. *Land* **2019**, *8*, 136. [[CrossRef](#)]
76. Atay Kaya, İ.; Kut Görgün, E. Land use and land cover change monitoring in Bandırma (Turkey) using remote sensing and geographic information systems. *Environ. Monit. Assess.* **2020**, *192*, 430. [[CrossRef](#)] [[PubMed](#)]

77. Sameer, M.K.; Hamid, A.M. Remote Sensing and GIS Techniques in Monitoring Land Use Land Cover Change. *Int. J. Sustain. Constr. Eng. Technol.* **2023**, *14*, 13–20. [[CrossRef](#)]
78. Kamel, M. Monitoring of land use and land cover change detection using multi-temporal remote sensing and time series analysis of qena-luxor governorates (QLGs), Egypt. *J. Indian Soc. Remote Sens.* **2020**, *48*, 1767–1785. [[CrossRef](#)]
79. Bashir, H.; Ahmad, S.S. Exploring geospatial techniques for spatiotemporal change detection in land cover dynamics along Soan River, Pakistan. *Environ. Monit. Assess.* **2017**, *189*, 222. [[CrossRef](#)] [[PubMed](#)]
80. Elagouz, M.; Abou-Shleel, S.; Belal, A.; El-Mohandes, M. Detection of land use/cover change in Egyptian Nile Delta using remote sensing. *Egypt. J. Remote Sens. Space Sci.* **2020**, *23*, 57–62. [[CrossRef](#)]
81. Löw, F.; Dimov, D.; Kenjabaev, S.; Zaitov, S.; Stulina, G.; Dukhovny, V. Land cover change detection in the Aralkum with multi-source satellite datasets. *GISci. Remote Sens.* **2022**, *59*, 17–35. [[CrossRef](#)]
82. Tikuye, B.G.; Rusnak, M.; Manjunatha, B.R.; Jose, J. Land Use and Land Cover Change Detection Using the Random Forest Approach: The Case of The Upper Blue Nile River Basin, Ethiopia. *Glob. Chall.* **2023**, *7*, 2300155. [[CrossRef](#)]
83. Yang, X.; Lv, Z.; Atli Benediktsson, J.; Chen, F. Novel Spatial–Spectral Channel Attention Neural Network for Land Cover Change Detection with Remote Sensed Images. *Remote Sens.* **2022**, *15*, 87. [[CrossRef](#)]
84. Panigrahi, S.; Verma, K.; Tripathi, P. Land cover change detection using focused time delay neural network. *Soft Comput.* **2019**, *23*, 7699–7713. [[CrossRef](#)]
85. Sefrin, O.; Riese, F.M.; Keller, S. Deep learning for land cover change detection. *Remote Sens.* **2020**, *13*, 78. [[CrossRef](#)]
86. Mou, L.; Zhu, X.X. A recurrent convolutional neural network for land cover change detection in multispectral images. In Proceedings of the IGARSS 2018—2018 IEEE International Geoscience and Remote Sensing Symposium, Valencia, Spain, 22–27 July 2018; pp. 4363–4366.
87. Zhu, Q.; Guo, X.; Deng, W.; Shi, S.; Guan, Q.; Zhong, Y.; Zhang, L.; Li, D. Land-use/land-cover change detection based on a Siamese global learning framework for high spatial resolution remote sensing imagery. *ISPRS J. Photogramm. Remote Sens.* **2022**, *184*, 63–78. [[CrossRef](#)]
88. Zhu, Y.; Jin, G.; Liu, T.; Zheng, H.; Zhang, M.; Liang, S.; Liu, J.; Li, L. Self-Attention and Convolution Fusion Network for Land Cover Change Detection over a New Data Set in Wenzhou, China. *Remote Sens.* **2022**, *14*, 5969. [[CrossRef](#)]
89. Lv, Z.; Zhong, P.; Wang, W.; You, Z.; Falco, N. Multi-scale Attention Network Guided with Change Gradient Image for Land Cover Change Detection Using Remote Sensing Images. *IEEE Geosci. Remote Sens. Lett.* **2023**, *20*, 2501805. [[CrossRef](#)]
90. Moncrieff, G.R. Continuous land cover change detection in a critically endangered shrubland ecosystem using neural networks. *Remote Sens.* **2022**, *14*, 2766. [[CrossRef](#)]
91. Wu, Y.; Li, L.; Wang, N.; Li, W.; Fan, J.; Tao, R.; Wen, X.; Wang, Y. CSTSUNet: A Cross Swin Transformer Based Siamese U-Shape Network for Change Detection in Remote Sensing Images. *IEEE Trans. Geosci. Remote Sens.* **2023**, *61*, 5623715. [[CrossRef](#)]
92. Hong, F.; He, G.; Wang, G.; Zhang, Z.; Peng, Y. Monitoring of Land Cover and Vegetation Changes in Juhugeng Coal Mining Area Based on Multi-Source Remote Sensing Data. *Remote Sens.* **2023**, *15*, 3439. [[CrossRef](#)]
93. Jing, R.; Gong, Z.; Guan, H. Land cover change detection with VHR satellite imagery based on multi-scale SLIC-CNN and SCAE features. *IEEE Access* **2020**, *8*, 228070–228087. [[CrossRef](#)]
94. Silveira, E.M.d.O.; Mello, J.M.d.; Acerbi Junior, F.W.; Carvalho, L.M.T.d. Object-based land-cover change detection applied to Brazilian seasonal savannahs using geostatistical features. *Int. J. Remote Sens.* **2018**, *39*, 2597–2619. [[CrossRef](#)]
95. Ding, L.; Zhu, K.; Peng, D.; Tang, H.; Guo, H. Adapting segment anything model for change detection in hr remote sensing images. *arXiv* **2023**, arXiv:2309.01429.
96. Zaidi, S.M.; Akbari, A.; Abu Samah, A.; Kong, N.S.; Gisen, A.; Isabella, J. Landsat-5 Time Series Analysis for Land Use/Land Cover Change Detection Using NDVI and Semi-Supervised Classification Techniques. *Pol. J. Environ. Stud.* **2017**, *26*, 2833–2840. [[CrossRef](#)]
97. Zhu, Y.; Li, Q.; Lv, Z.; Falco, N. Novel Land Cover Change Detection Deep Learning Framework with Very Small Initial Samples Using Heterogeneous Remote Sensing Images. *Preprints* **2023**, 2023060682.. [[CrossRef](#)]
98. Seydi, S.T.; Hasanlou, M. A new land-cover match-based change detection for hyperspectral imagery. *Eur. J. Remote Sens.* **2017**, *50*, 517–533. [[CrossRef](#)]
99. Lv, Z.; Huang, H.; Sun, W.; Jia, M.; Benediktsson, J.A.; Chen, F. Iterative Training Sample Augmentation for Enhancing Land Cover Change Detection Performance with Deep Learning Neural Network. *IEEE Trans. Neural Netw. Learn. Syst.* **2023**. [[CrossRef](#)] [[PubMed](#)]
100. Peng, D.; Bruzzone, L.; Zhang, Y.; Guan, H.; Ding, H.; Huang, X. SemiCDNet: A semisupervised convolutional neural network for change detection in high resolution remote-sensing images. *IEEE Trans. Geosci. Remote Sens.* **2020**, *59*, 5891–5906. [[CrossRef](#)]
101. Zhang, X.; Shi, W.; Lv, Z.; Peng, F. Land cover change detection from high-resolution remote sensing imagery using multitemporal deep feature collaborative learning and a semi-supervised chan–vese model. *Remote Sens.* **2019**, *11*, 2787. [[CrossRef](#)]
102. Sapucci, G.R.; Negri, R.G.; Casaca, W.; Massi, K.G. Analyzing spatio-temporal land cover dynamics in an atlantic forest portion using unsupervised change detection techniques. *Environ. Model. Assess.* **2021**, *26*, 581–590. [[CrossRef](#)]
103. Wang, Y.; Zhao, F.; Chen, P. A framework of spatiotemporal fuzzy clustering for land-cover change detection using SAR time series. *Int. J. Remote Sens.* **2017**, *38*, 450–466. [[CrossRef](#)]
104. Häme, T.; Sirro, L.; Kilpi, J.; Seitsonen, L.; Andersson, K.; Melkas, T. A hierarchical clustering method for land cover change detection and identification. *Remote Sens.* **2020**, *12*, 1751. [[CrossRef](#)]

105. Espinoza-Molina, D.; Bahmanyar, R.; Díaz-Delgado, R.; Bustamante, J.; Datcu, M. Land-cover change detection using local feature descriptors extracted from spectral indices. In Proceedings of the 2017 IEEE International Geoscience and Remote Sensing Symposium (IGARSS), Fort Worth, TX, USA, 23–28 July 2017; pp. 1938–1941.
106. Hu, Y.; Raza, A.; Syed, N.R.; Acharki, S.; Ray, R.L.; Hussain, S.; Dehghanisanij, H.; Zubair, M.; Elbeltagi, A. Land Use/Land Cover Change Detection and NDVI Estimation in Pakistan’s Southern Punjab Province. *Sustainability* **2023**, *15*, 3572. [[CrossRef](#)]
107. Bhattacharjee, S.; Islam, M.T.; Kabir, M.E.; Kabir, M.M. Land-use and land-cover change detection in a north-eastern wetland ecosystem of Bangladesh using remote sensing and GIS techniques. *Earth Syst. Environ.* **2021**, *5*, 319–340. [[CrossRef](#)]
108. Kaldane, H.; Turkar, V.; De, S.; Shitole, S.; Deo, R. Land Cover Change Detection for Fully Polarimetric SAR Images. In Proceedings of the 2019 URSI Asia-Pacific Radio Science Conference (AP-RASC), New Delhi, India, 9–15 March 2019; pp. 1–4.
109. Liu, B.; Chen, J.; Chen, J.; Zhang, W. Land cover change detection using multiple shape parameters of spectral and NDVI curves. *Remote Sens.* **2018**, *10*, 1251. [[CrossRef](#)]
110. Viana, C.M.; Girão, I.; Rocha, J. Long-term satellite image time-series for land use/land cover change detection using refined open source data in a rural region. *Remote Sens.* **2019**, *11*, 1104. [[CrossRef](#)]
111. Zhang, Y.; Zhao, H. Land-use and land-cover change detection using dynamic time warping-based time series clustering method. *Can. J. Remote Sens.* **2020**, *46*, 67–83. [[CrossRef](#)]
112. He, D.; Zhong, Y.; Zhang, L. Spectral-spatial-temporal MAP-based sub-pixel mapping for land-cover change detection. *IEEE Trans. Geosci. Remote Sens.* **2019**, *58*, 1696–1717. [[CrossRef](#)]
113. Wang, J.; Yang, M.; Chen, Z.; Lu, J.; Zhang, L. An MLC and U-Net integrated method for Land Use/Land Cover Change detection based on time series NDVI-composed image from PlanetScope satellite. *Water* **2022**, *14*, 3363. [[CrossRef](#)]
114. Yan, J.; Wang, L.; He, H.; Liang, D.; Song, W.; Han, W. Large-area land-cover changes monitoring with time-series remote sensing images using transferable deep models. *IEEE Trans. Geosci. Remote Sens.* **2022**, *60*, 4409917. [[CrossRef](#)]
115. Fang, W.; Xi, C. Land-cover change detection for SAR images based on biobjective fuzzy local information clustering method with decomposition. *IEEE Geosci. Remote Sens. Lett.* **2022**, *19*, 4506105. [[CrossRef](#)]
116. Lv, Z.; Shi, W.; Zhou, X.; Benediktsson, J.A. Semi-automatic system for land cover change detection using bi-temporal remote sensing images. *Remote Sens.* **2017**, *9*, 1112. [[CrossRef](#)]
117. Lv, Z.; Liu, T.; Shi, C.; Benediktsson, J.A. Local histogram-based analysis for detecting land cover change using VHR remote sensing images. *IEEE Geosci. Remote Sens. Lett.* **2020**, *18*, 1284–1287. [[CrossRef](#)]
118. Lv, Z.Y.; Liu, T.F.; Zhang, P.; Benediktsson, J.A.; Lei, T.; Zhang, X. Novel adaptive histogram trend similarity approach for land cover change detection by using bitemporal very-high-resolution remote sensing images. *IEEE Trans. Geosci. Remote Sens.* **2019**, *57*, 9554–9574. [[CrossRef](#)]
119. Cardama, F.J.; Heras, D.B.; Argüello, F. Consensus Techniques for Unsupervised Binary Change Detection Using Multi-Scale Segmentation Detectors for Land Cover Vegetation Images. *Remote Sens.* **2023**, *15*, 2889. [[CrossRef](#)]
120. Zheng, Z.; Cao, J.; Lv, Z.; Benediktsson, J.A. Spatial-spectral feature fusion coupled with multi-scale segmentation voting decision for detecting land cover change with VHR remote sensing images. *Remote Sens.* **2019**, *11*, 1903. [[CrossRef](#)]
121. Xing, J.; Sieber, R.; Caelli, T. A scale-invariant change detection method for land use/cover change research. *ISPRS J. Photogramm. Remote Sens.* **2018**, *141*, 252–264. [[CrossRef](#)]
122. Lv, Z.; Wang, F.; Liu, T.; Kong, X.; Benediktsson, J.A. Novel automatic approach for land cover change detection by using VHR remote sensing images. *IEEE Geosci. Remote Sens. Lett.* **2021**, *19*, 8016805. [[CrossRef](#)]
123. Lv, Z.; Liu, T.; Zhang, P.; Atli Benediktsson, J.; Chen, Y. Land cover change detection based on adaptive contextual information using bi-temporal remote sensing images. *Remote Sens.* **2018**, *10*, 901. [[CrossRef](#)]
124. Naik, N.; Chandrasekaran, K.; Meenakshi Sundaram, V.; Panner, P. Spatio-temporal analysis of land use/land cover change detection in small regions using self-supervised lightweight deep learning. *Stoch. Environ. Res. Risk Assess.* **2023**, *37*, 5029–5049. [[CrossRef](#)]
125. Zhang, C.; Wei, S.; Ji, S.; Lu, M. Detecting large-scale urban land cover changes from very high resolution remote sensing images using CNN-based classification. *ISPRS Int. J. Geo-Inf.* **2019**, *8*, 189. [[CrossRef](#)]
126. Song, F.; Yang, Z.; Gao, X.; Dan, T.; Yang, Y.; Zhao, W.; Yu, R. Multi-scale feature based land cover change detection in mountainous terrain using multi-temporal and multi-sensor remote sensing images. *IEEE Access* **2018**, *6*, 77494–77508. [[CrossRef](#)]
127. Seydi, S.T.; Shah-Hosseini, R.; Amani, M. A Multi-Dimensional Deep Siamese Network for Land Cover Change Detection in Bi-Temporal Hyperspectral Imagery. *Sustainability* **2022**, *14*, 12597. [[CrossRef](#)]
128. Prasad, J.; Sreelatha, M.; SuvarnaVani, K. V-BANet: Land cover change detection using effective deep learning technique. *Ecol. Inform.* **2023**, *75*, 102019. [[CrossRef](#)]
129. Luo, K.; Li, B.; Moiwo, J.P. Monitoring Land-Use/Land-Cover changes at a provincial large scale using an object-oriented technique and medium-resolution remote-sensing images. *Remote Sens.* **2018**, *10*, 2012. [[CrossRef](#)]
130. Zhu, J.; Su, Y.; Guo, Q.; Harmon, T.C. Unsupervised object-based differencing for land-cover change detection. *Photogramm. Eng. Remote Sens.* **2017**, *83*, 225–236. [[CrossRef](#)]
131. Wang, Z.; Liu, Y.; Ren, Y.; Ma, H. Object-Level Double Constrained Method for Land Cover Change Detection. *Sensors* **2018**, *19*, 79. [[CrossRef](#)] [[PubMed](#)]

132. Shi, S.; Zhong, Y.; Zhao, J.; Lv, P.; Liu, Y.; Zhang, L. Land-use/land-cover change detection based on class-prior object-oriented conditional random field framework for high spatial resolution remote sensing imagery. *IEEE Trans. Geosci. Remote Sens.* **2020**, *60*, 5600116. [[CrossRef](#)]
133. Amitrano, D.; Guida, R.; Iervolino, P. Semantic unsupervised change detection of natural land cover with multitemporal object-based analysis on SAR images. *IEEE Trans. Geosci. Remote Sens.* **2020**, *59*, 5494–5514. [[CrossRef](#)]
134. Lv, Z.; Liu, T.; Benediktsson, J.A. Object-oriented key point vector distance for binary land cover change detection using VHR remote sensing images. *IEEE Trans. Geosci. Remote Sens.* **2020**, *58*, 6524–6533. [[CrossRef](#)]
135. Xiao, T.; Wan, Y.; Chen, J.; Shi, W.; Qin, J.; Li, D. Multiresolution-Based Rough Fuzzy Possibilistic-Means Clustering Method for Land Cover Change Detection. *IEEE J. Sel. Top. Appl. Earth Obs. Remote Sens.* **2022**, *16*, 570–580. [[CrossRef](#)]
136. Himeur, Y.; Alsalemi, A.; Bensaali, F.; Amira, A. A novel approach for detecting anomalous energy consumption based on micro-moments and deep neural networks. *Cogn. Comput.* **2020**, *12*, 1381–1401. [[CrossRef](#)]
137. Tharwat, A. Classification assessment methods. *Appl. Comput. Inform.* **2020**, *17*, 168–192. [[CrossRef](#)]
138. Kerr, G.H.; Fischer, C.; Reulke, R. Reliability assessment for remote sensing data: Beyond Cohen’s kappa. In Proceedings of the 2015 IEEE International Geoscience and Remote Sensing Symposium (IGARSS), Milan, Italy, 26–31 July 2015; pp. 4995–4998.
139. Youssef, R.; Aniss, M.; Jamal, C. Machine learning and deep learning in remote sensing and urban application: A systematic review and meta-analysis. In Proceedings of the 4th Edition of International Conference on Geo-IT and Water Resources 2020, Geo-IT and Water Resources 2020, Al Hoceima, Morocco, 11–12 March 2020; pp. 1–5.
140. Arrieta, A.B.; Díaz-Rodríguez, N.; Del Ser, J.; Bennetot, A.; Tabik, S.; Barbado, A.; García, S.; Gil-López, S.; Molina, D.; Benjamins, R.; et al. Explainable Artificial Intelligence (XAI): Concepts, taxonomies, opportunities and challenges toward responsible AI. *Inf. Fusion* **2020**, *58*, 82–115. [[CrossRef](#)]
141. Szostak, M.; Pietrzykowski, M.; Likus-Ciešlik, J. Reclaimed area land cover mapping using Sentinel-2 Imagery and LiDAR Point Clouds. *Remote Sens.* **2020**, *12*, 261. [[CrossRef](#)]
142. Salah, M. Filtering of remote sensing point clouds using fuzzy C-means clustering. *Appl. Geomat.* **2020**, *12*, 307–321. [[CrossRef](#)]
143. Tseng, Y.H.; Wang, C.K.; Chu, H.J.; Hung, Y.C. Waveform-based point cloud classification in land-cover identification. *Int. J. Appl. Earth Obs. Geoinf.* **2015**, *34*, 78–88. [[CrossRef](#)]
144. Zhou, K.; Ming, D.; Lv, X.; Fang, J.; Wang, M. CNN-based land cover classification combining stratified segmentation and fusion of point cloud and very high-spatial resolution remote sensing image data. *Remote Sens.* **2019**, *11*, 2065. [[CrossRef](#)]

**Disclaimer/Publisher’s Note:** The statements, opinions and data contained in all publications are solely those of the individual author(s) and contributor(s) and not of MDPI and/or the editor(s). MDPI and/or the editor(s) disclaim responsibility for any injury to people or property resulting from any ideas, methods, instructions or products referred to in the content.